



Formation of a PSI–PSII megacomplex containing LHCSR and PsbS in the moss *Physcomitrella patens*

Ryo Furukawa¹ · Michiki Aso¹ · Tomomichi Fujita² · Seiji Akimoto³ · Ryouichi Tanaka¹ · Ayumi Tanaka¹ · Makio Yokono^{1,4} · Atsushi Takabayashi¹

Received: 27 June 2019 / Accepted: 8 September 2019 / Published online: 20 September 2019
© The Botanical Society of Japan and Springer Japan KK, part of Springer Nature 2019

Abstract

Mosses are one of the earliest land plants that diverged from fresh-water green algae. They are considered to have acquired a higher capacity for thermal energy dissipation to cope with dynamically changing solar irradiance by utilizing both the “algal-type” light-harvesting complex stress-related (LHCSR)-dependent and the “plant-type” PsbS-dependent mechanisms. It is hypothesized that the formation of photosystem (PS) I and II megacomplex is another mechanism to protect photosynthetic machinery from strong irradiance. Herein, we describe the analysis of the PSI–PSII megacomplex from the model moss, *Physcomitrella patens*, which was resolved using large-pore clear-native polyacrylamide gel electrophoresis (lpCN-PAGE). The similarity in the migration distance of the *Physcomitrella* PSI–PSII megacomplex to the Arabidopsis megacomplex shown during lpCN-PAGE suggested that the *Physcomitrella* PSI–PSII and Arabidopsis megacomplexes have similar structures. Time-resolved chlorophyll fluorescence measurements show that excitation energy was rapidly and efficiently transferred from PSII to PSI, providing evidence of an ordered association of the two photosystems. We also found that LHCSR and PsbS co-migrated with the *Physcomitrella* PSI–PSII megacomplex. The megacomplex showed pH-dependent chlorophyll fluorescence quenching, which may have been induced by LHCSR and/or PsbS proteins with the collaboration of zeaxanthin. We discuss the mechanism that regulates the energy distribution balance between two photosystems in *Physcomitrella*.

Keywords *Physcomitrella* · PSI–PSII megacomplex · LHCSR · CN-PAGE

Introduction

Plants contain photosystems that absorb light energy and transfer it to the reaction center to drive photosynthetic

electron transfer. Oxygenic photosynthesis requires the cooperative work of two photosystems (PSI and PSII); therefore, the regulation of excitation energy distribution between PSI and PSII is important to enable plants to avoid photooxidative damage (Minagawa and Tokutsu 2015; Niyogi and Truong 2013; Ruban 2015; Xu et al. 2015; Wobbe et al. 2016). Therefore, rapid mechanisms for the fine-tuning of energy distribution between these two photosystems are essential for adaption to terrestrial environments, where the intensity of sunlight dynamically fluctuates, even over the short term (Minagawa and Tokutsu 2015; Ruban 2015; Xu et al. 2015). One such mechanism is non-photochemical quenching (NPQ), which enables PSII to dissipate excess light energy harmlessly as heat (Goss and Lepetit 2015; Minagawa and Tokutsu 2015; Niyogi and Truong 2013; Ruban 2015, 2016; Wobbe et al. 2016; Xu et al. 2015). NPQ is induced and relaxed, depending on the pH gradient across thylakoid membranes, from within seconds to minutes. State transition during photosynthesis is another mechanism that rapidly regulates the excitation energy distribution between the two photosystems by the reversible allocation

Electronic supplementary material The online version of this article (<https://doi.org/10.1007/s10265-019-01138-2>) contains supplementary material, which is available to authorized users.

✉ Makio Yokono
filia@mac.com

Atsushi Takabayashi
takabayashi@pop.lowtem.hokudai.ac.jp

¹ Institute of Low-Temperature Science, Hokkaido University, N19 W8 Kita-ku, Sapporo 060-0819, Japan

² Faculty of Science, Hokkaido University, N10 W8 Kita-ku, Sapporo 060-0810, Japan

³ Graduate School of Science, Kobe University, Kobe 657-8501, Japan

⁴ Innovation Center, Nippon Flour Mills Co., Ltd., Atsugi 243-0041, Japan

of the light-harvesting complex II (LHCII) between them (Minagawa and Tokutsu 2015; Wobbe et al. 2016; Xu et al. 2015). This transition is regulated by the phosphorylation of mobile LHCII, which is performed by redox-active kinases (Bellafiore et al. 2005; Pesaresi et al. 2009). The induction and relaxation of the state transition can also occur within minutes.

In addition to NPQ and state transition, the spillover of excitation energy between the two photosystems can contribute to the regulation of the balance of energy distribution between them. First, Järvi et al. (2011) reported the presence of large protein complexes comprising both PSI and PSII in *Arabidopsis thaliana* (hereafter *Arabidopsis*). Additionally, Yokono et al. (2015) provided spectrochemical evidence showing that the excitation energy can be shared between the two photosystems in the *Arabidopsis* PSI–PSII megacomplexes. It is also hypothesized that the megacomplex is formed in the marginal region of the appressed grana membranes, where PSI and PSII are present (Suorsa et al. 2014). In addition to *Arabidopsis*, PSI–PSII megacomplex formation was also reported in an early-branched vascular plant *Selaginella martensii* (Ferroni et al. 2016) and a green alga *Neochloris oleoabundans* (Giovanardi et al. 2017). Furthermore, the spillover from PSII to PSI can be observed in a wide variety of green plants, including green algae (Yokono et al. 2019). These findings showed that the spillover within the PSI–PSII megacomplex occur widely in the green lineage. The amount of the PSI–PSII megacomplex may rapidly change, depending on light conditions, which contributes to the regulation of energy distribution between PSI and PSII (Ferroni et al. 2016; Suorsa et al. 2015; Yokono et al. 2015).

The moss, *Physcomitrella patens* (Hedw.) (hereafter *Physcomitrella*), is a model plant for understanding the evolutionary changes in photosystems from green algae to land plants. It belongs to an early terrestrial group in the green lineage and displays photosynthetic regulation characteristics intermediate between green algae and higher plants (Niyogi and Truong 2013). Specifically, *Physcomitrella* possesses both PsbS- and LHCSR-dependent NPQ (Iwai and Yokono 2017; Niyogi and Truong 2013; Peers et al. 2009). To date, PsbS- and LHCSR-dependent NPQ have been reported in the green lineage (Niyogi and Truong 2013; Peers et al. 2009). Higher plants only possess PsbS-dependent energy-dependent (qE) quenching because they have lost the LHCSR protein during evolution (Niyogi and Truong 2013). Although green algae possess both PsbS- and LHCSR-dependent NPQ, LHCSR-dependent NPQ is the primary NPQ in green algae. A recent study (Correa-Galvis et al. 2016a, b) reported that *Chlamydomonas reinhardtii* (hereafter *Chlamydomonas*) PsbS is required to activate the LHCSR-dependent NPQ,

suggesting that PsbS works cooperatively with LHCSR in green algae. In contrast, in *Physcomitrella*, the sub-thylakoid localization of PsbS is different from that of LHCSR (Pinnola et al. 2015). A single loss of PsbS or LHCSR leads to a similar decrease in NPQ, while the simultaneous loss of PsbS and LHCSR proteins reduced NPQ to almost zero (Alboresi et al. 2010; Gerotto et al. 2011). In addition, the mutant plants lacking both PsbS and LHCSR were more susceptible to high light intensities than the single mutant (Alboresi et al. 2010). These data showed that both PsbS and LHCSR have an essential role in NPQ in *Physcomitrella*. In this sense, *Physcomitrella* has an intermediate characteristic for the NPQ that is different from green algae and higher plants. Furthermore, *Physcomitrella* has a strong capacity to dissipate excess light energy as heat, because both PsbS- and LHCSR-dependent NPQ occurred additively (Alboresi et al. 2010). This should contribute to the early adaptation to the strong and fluctuating light conditions in the terrestrial environment (Alboresi et al. 2010).

In the present study, we demonstrate the presence of the PSI–PSII megacomplex in the protonemata of *P. patens*, which can share excitation energy between the two photosystems. The megacomplex possesses low-energy chlorophylls in PSI–LHCI, similar to higher plants (Yokono et al. 2015). Low-energy chlorophylls can mediate P700⁺ quenching (Croce and van Amerongen 2013) and may possibly mediate zeaxanthin-dependent quenching (Ballottari et al. 2014). In addition, the megacomplex showed a pH-dependent quenching ability, most likely due to its interaction with LHCSR and PsbS, which can contribute to the early adaptation to the strong and fluctuating light conditions in the terrestrial environment.

Materials and methods

Plant materials

Physcomitrella patens protonemata were cultured on a layer of cellophane overlaid on BCDAT (BCD medium (Nishiyama et al. 2000) supplemented with 1 mM CaCl₂ and 5 mM di-ammonium [+-]tartrate) solidified with 0.8% (w/v) agar at 25 °C under continuous light (40 μmol photons m⁻² s⁻¹). Four-day-old cultured protonemata were used as the low-light sample. Several of the 4-day-old cultured protonemata were further illuminated with strong light (500 μmol photons m⁻² s⁻¹) for 1 h with cold spot fiber optics (PCS-UMX250, NPI, Tokyo, Japan), and were used as the strong light sample.

Isolation of thylakoid membranes

The isolation of thylakoid membranes was performed largely according to the method described by Järvi et al. (2011). All procedures were performed on ice or at 4 °C. The protonemata were suspended in a grinding buffer [50 mM Hepes/KOH (pH 7.5), 330 mM sorbitol, 2 mM EDTA, 1 mM MgCl₂, 5 mM ascorbate, 0.05% BSA, 10 mM sodium fluoride, and 0.25 mg mL⁻¹ Pefabloc (Sigma-Aldrich, St. Louis, MO, USA)]. Approximately 1 mL of the suspension was transferred to a 2 mL vial containing 1 g of glass beads (0.5 mm diameter) and the protonemata were disrupted by three × 10 s-disruption treatments using a Mini-Bead Beater (Waken B Tech Co., Ltd, Kyoto, Japan). The homogenate was immediately centrifuged at 5,000×g for 4 min at 4 °C and resuspended in a shock buffer (50 mM Hepes/KOH (pH 7.5), 5 mM sorbitol, 5 mM MgCl₂, and 10 mM sodium fluoride). After centrifugation at 5,000×g for 4 min at 4 °C, the pellet was resuspended in a storage buffer (50 mM Hepes/KOH (pH 7.5), 100 mM sorbitol, 10 mM MgCl₂, and 10 mM sodium fluoride) at a concentration of 1.5 mg mL⁻¹ chlorophyll.

Clear-native (CN)-PAGE

CN-PAGE was performed in accordance with the methodology used by Umetani et al. (2018). The isolated thylakoid membranes were resuspended in a solubilization buffer (50 mM imidazole/HCl (pH 7.0), 20% glycerol, 5 mM 6-aminocaproic acid, and 1 mM EDTA). An equal volume of 2% α-dodecyl maltoside (DM) and 0.01-volumes of protease inhibitor cocktail (Sigma-Aldrich, St. Louis, MO, USA) were added to the resuspended thylakoids and the chlorophyll-protein complexes were solubilized on ice for 1 min. Insoluble material was removed from the samples by centrifugation at 21,600×g at 4 °C for 1 min. After the addition of a 0.5-volumes of 20 mg mL⁻¹ amphipol A8-35 (Anatrace, OH, USA) to the supernatant, the samples were separated on 4–13% polyacrylamide gradient gels at 4 °C using an anode buffer [50 mM imidazole/HCl (pH 7.0 at 4 °C)] and a cathode buffer [50 mM Tricine and 15 mM imidazole/HCl (pH 7.0 at 4 °C)].

Large-pore (lp)CN-PAGE

The lpCN-PAGE was performed using the procedure described by Järvi et al. (2011). A 25BTH20G buffer (25 mM BisTris/HCl (pH 7.0), 20% (w/v) glycerol, and 0.25 mg mL⁻¹ Pefabloc) was added to the thylakoid membrane suspension to achieve a concentration of 1 mg mL⁻¹ chlorophyll. To solubilize the thylakoid protein complexes with digitonin, an equal volume of 2% digitonin in the 25BTH20G buffer was added to the thylakoid suspension

and incubated at 20 °C in the dark for 5 min with continuous stirring. After centrifugation to remove insoluble materials, a 1/6 volume of 20 mg mL⁻¹ amphipol A8-35 (Anatrace, OH, USA) was added to the supernatant. The samples were loaded onto lpCN gels immediately after the solubilization process. The separation gels contained 3.5–13% (w/v) polyacrylamide, which is composed of acrylamide and bisacrylamide in the ratio of 29:1. The sample gels contained 3% polyacrylamide, which is composed of acrylamide and bisacrylamide in a ratio of 4:1. Electrophoresis was performed using an anode buffer [50 mM BisTris/HCl (pH 7.0 at 4 °C)] and a cathode buffer (50 mM Tricine, 15 mM BisTris/HCl (pH 7.0 at 4 °C), and 0.01% amphipol A8-35).

Two-dimensional lpCN/SDS-PAGE

Two-dimensional (2D)-lpCN/SDS-PAGE was performed using the procedure described by Umetani et al. (2018). Proteins in an lpCN-PAGE gel strip were denatured in a solubilization buffer (1% SDS and 1% 2-mercaptoethanol) for 60 min at 30 °C and separated on a 14% acrylamide gel containing 4 M urea, using the Laemmli system. Silver-staining was performed using the Pierce Silver Stain kit (ThermoFisher Scientific, Rockford, IL, USA), according to the manufacturer's instructions.

Immunoblotting

The separated proteins were transferred to a polyvinylidene fluoride membrane (PolyScreen PVDF transfer membrane, PerkinElmer Life Sciences, MA, USA) and detected by using specific antibodies and a Western Lightning Plus-ECL (PerkinElmer Life science, MA, USA). All antibodies used in the present study were purchased from Agrisera (Vännäs, Sweden). Anti-PsbB (AS04 038) and anti-PsbC antibodies (AS11 1787) were used for detection of PSII core subunits. Anti-PsaD antibodies (AS09 461) were used to detect a core subunit of PSI. Anti-Lhcb2 (AS01 003) and Lhcb3 (AS01 002) antibodies were used to detect the major LHCI proteins. Anti-LHCSR1 antibodies (AS15 3081) were used for the detection of an LHCSR protein.

Spectroscopic analyses

Time-resolved fluorescence measurements and analysis were performed at pH 7 and pH 4.5 by using the PSI–PSII megacomplexes from the control and the 1 h-strong light illuminated plants, as described by Yokono et al. (2015). The PSI–PSII megacomplex in the lpCN gel was soaked for 5 min at 4 °C using a buffer containing 50 mM BisTris/HCl (pH 7 or pH 4.5) and 0.5 M 6-aminocaproic acid. The excitation wavelength was 408 nm and the repetition rate was 2 MHz, which did not interfere with measurements

up to 100 ns (24.4 ps per channel \times 4,096 channels). To improve the time resolution, time-resolved fluorescence was also measured up to 10 ns (2.4 ps per channel \times 4,096 channels). After a global analysis of the fluorescence kinetics, fluorescence decay-associated spectra were constructed. Steady-state fluorescence spectra were measured by using an F-2500 spectrophotometer (Hitachi). The optical slit widths for excitation and emission were 10 and 2.5 nm, respectively. Steady-state absorption spectra at room temperature (20–25 °C) were measured based on the methodology described by Umetani et al. (2018).

Pigment determination

To extract pigments, *Physcomitrella* protonemata cells were homogenized in acetone with stainless beads (5 mm in diameter, TCS0-0100, Bio medical science, Tokyo) for 1 min using the ShakeMaster bead shaker (BioMedical Science Co. Ltd, Tokyo, Japan). The homogenates were centrifuged at 21,600 \times g for 5 min, and the supernatant was loaded onto a C18 column (YMC AL303 250 \times 4.6 mm, 5 μ m, YMC Co., Ltd., Kyoto, Japan). The sample was eluted with an isocratic flow of solvent A (100% methanol) for 17 min, followed by a linear gradient from solvent A to B (60% methanol, 20% ethanol, 20% hexane) in 5 min and with an isocratic flow of solvent B at a flow rate of 0.8 mL/min. The eluates were monitored by a L-2450 photodiode array detector (HITACHI High Technologies Science Corporation, Tokyo, Japan) at 450 nm. The pigments were identified and quantified by comparing their absorption spectra with relevant standard pigments.

Results

Isolation of a *Physcomitrella* PSI–PSII megacomplex by lpCN-PAGE

The PSI–PSII megacomplex is one of the largest known plant complexes and is estimated to be larger than 3,000 kDa (calculated based on the structural model of the Arabidopsis megacomplex in Yokono et al. 2019). Only a few techniques currently exist that can resolve the size of the complex—such as size-exclusion chromatography and sucrose-density gradient centrifugation. To the best of our knowledge, only native PAGE systems have been successful in resolving the PSI–PSII megacomplex thus far (Ferroni et al. 2016; Giovanardi et al. 2017; Järvi et al. 2011; Yokono et al. 2015). Moreover, standard blue-native (BN) and clear-native (CN)-PAGE systems cannot be used to isolate the PSI–PSII megacomplex because it is too large to enter the separation gel and must, therefore, remain in the sample gel (Järvi et al. 2011). Therefore, for this study, we used large-pore

CN-PAGE (lpCN-PAGE)—a process that consists of using large-pore acrylamide gel that allows the separation of the megacomplex from the rest of the photosynthetic complexes and the insolubilized thylakoid membranes.

We began by solubilizing the thylakoid protein complexes using digitonin from cells grown under low-light conditions and from cells illuminated with strong light for 1 h. DOC is typically used to provide the negative charge required to separate the solubilized protein complexes by lpCN-PAGE at a neutral pH. However, we replaced DOC with amphipol A8-35 for this study.

Amphipols are a new class of amphipathic polymer that enable protein complexes to enhance their stability in detergent-free solutions. Amphipol A8-35, in particular, has been widely used in the stabilization of membrane proteins (Popot et al. 2011; Watanabe et al. 2019). As a result of using this technique, we succeeded in resolving several pigment-protein complexes (Fig. 1). As far as we know, this is the first study demonstrating the use of lpCN-PAGE using amphipols. Based on 2D-lpCN/SDS-PAGE, immunoblotting analysis (Fig. 2), and silver-staining (Fig. S1), the three major pigment-protein bands resolved by lpCN-PAGE were identified as a PSI–PSII megacomplex, a PSI–LHCI and PSII dimer, and an LHCII trimer, respectively. The PSII–LHCII was not clearly observed, because the grana core where the PSII–LHCII is mostly localized, is only partially solubilized by digitonin. Passing the PSI–PSII megacomplex band through the sample gel during lpCN-PAGE showed that it was a protein complex rather than insufficiently solubilized membrane particles. The *Physcomitrella* PSI–PSII megacomplex contained PSI, PSII, and LHCII proteins (Fig. 2), as found in the Arabidopsis megacomplex (Yokono et al. 2015). The molecular weights of the PSI–LHCI and PSII dimer were typically quite similar, which resulted in similar migration distances (Fig. 1). Smaller PSI–PSII complexes, which had similar migration distances, might be present in the band (Yokono et al. 2015), although no further analysis was conducted in the present study.

Recently, we reported a structural model of the Arabidopsis PSI–PSII megacomplex, based on the negatively-stained particles observed by electron microscopy (Yokono et al. 2019). In this model, one PSII dimer was sandwiched by two PSI–LHCI complexes with two-fold rotational symmetry, and additional LHCII trimers surrounded peripherally. If the *Physcomitrella* PSI–PSII megacomplex had a similar structure to this model, its molecular size should be similar to that of the Arabidopsis megacomplex. To compare the molecular sizes of the *Physcomitrella* PSI–PSII megacomplex and the Arabidopsis megacomplex, we resolved the digitonin-solubilized thylakoid protein complexes from Arabidopsis and *Physcomitrella* by lpCN-PAGE using different acrylamide concentrations (3–13% and 3.25–13%) (Fig. 3). The subunit compositions of the *Physcomitrella* PSI–PSII

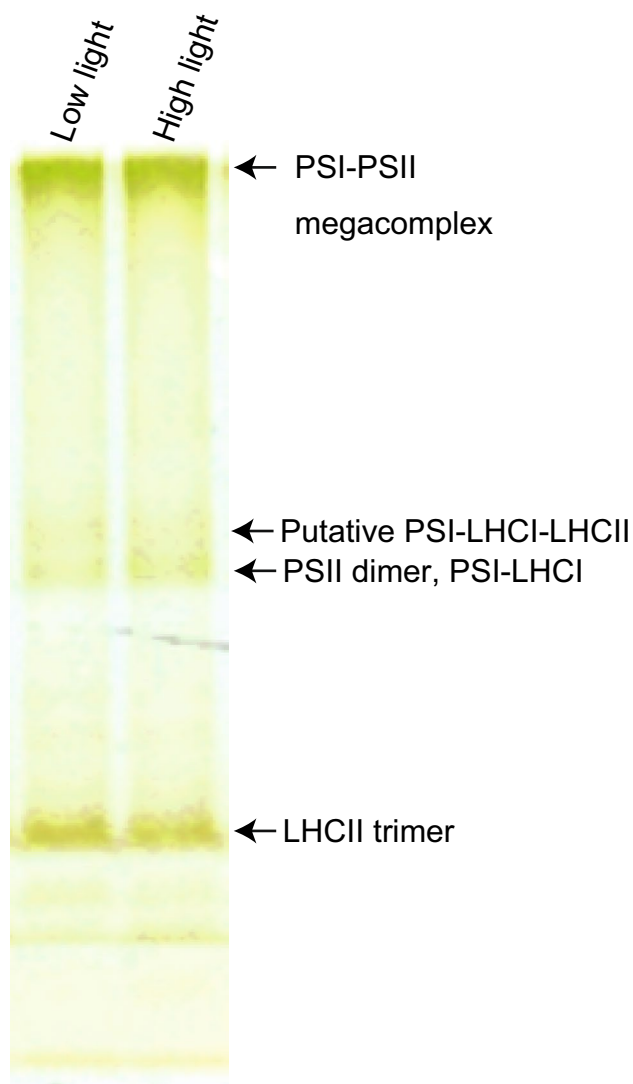


Fig. 1 Separation of thylakoid pigment-protein complexes in *Physcomitrella* by IpCN-PAGE with Amphipol A8-35. The thylakoid membrane proteins from the protonemata cells grown under low-light ($40 \mu\text{mol photons m}^{-2} \text{s}^{-1}$) conditions and the cells illuminated under strong light ($500 \mu\text{mol photons m}^{-2} \text{s}^{-1}$) for 1 h were solubilized with 1% digitonin and were separated by 3.5–13% polyacrylamide

megacomplexes resolved by the two different gels [3.5–13% (Fig. 1) and 3.25–13% (Fig. 3)] appeared almost identical, based on the silver-stained 2D-IpCN/SDS-PAGE (Figs. S1, S2). The green band, other than the PSI–PSII megacomplex, did not appear around it even when the gel concentrations were altered (Figs. 1, 3). This supports the hypothesis that band contamination, such as PSII–LHCII megacomplexes, was negligible. On the other hand, the PSI–PSII megacomplex band appeared somewhat smeared (Figs. 1, 3). This is most likely due to the structural heterogeneity of the megacomplex, which includes the varied binding patterns of peripheral LHCII to the PSI–PSII megacomplex as shown and discussed by Yokono et al. (2019). The migration

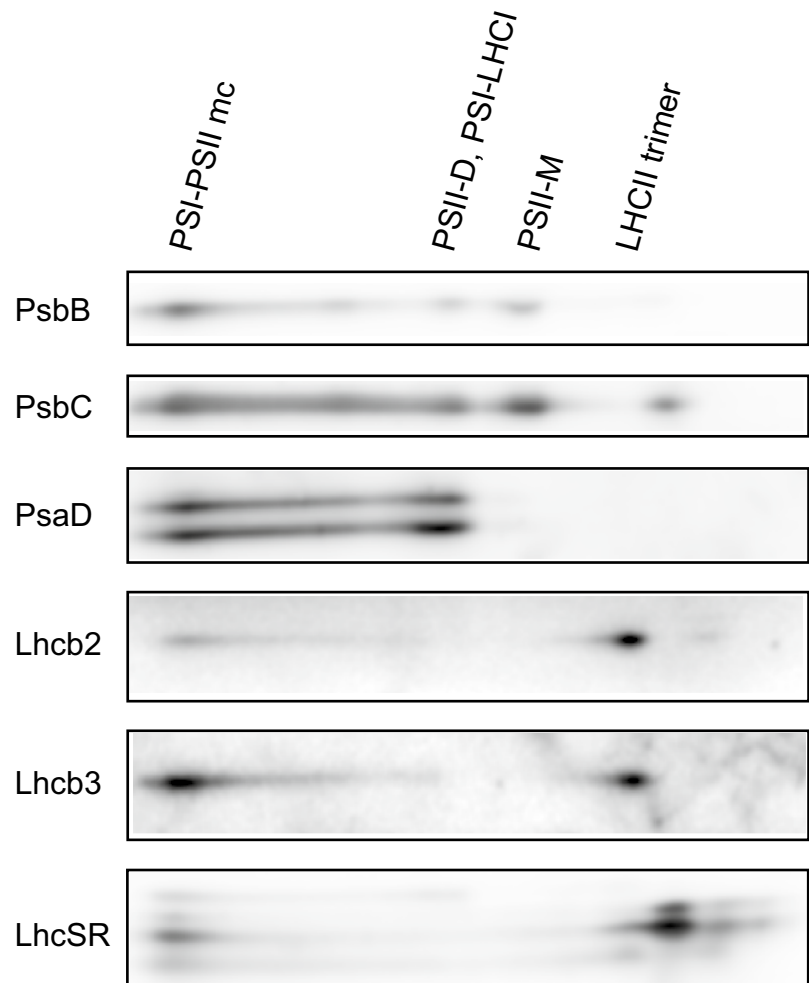
distances of the *Physcomitrella* PSI–PSII megacomplexes were similar to those of Arabidopsis, which demonstrated that the molecular mass of the PSI–PSII megacomplexes in Arabidopsis and *Physcomitrella* were similar to each other (Fig. 3). These data suggested that the structure of the *Physcomitrella* PSI–PSII megacomplex is similar to that of the Arabidopsis PSI–PSII megacomplex.

LHCSR is involved in the NPQ formation of both PSI and PSII in *Physcomitrella*, though the protein is localized in the stroma lamellae and grana margin, where PSII is scarcely distributed (Pinnola et al. 2015). As the PSI–PSII megacomplex likely localizes in the stroma lamellae, we hypothesized that LHCSR binds to the PSI–PSII megacomplex and dissipates the absorbed energy as heat. To verify this hypothesis, we further performed immunoblotting analysis of LHCSR after 2D-IpCN/SDS-PAGE using anti-LHCSR antibodies (Fig. 2). The results showed that LHCSR co-migrated in the PSI–PSII megacomplex, in addition to their monomeric form, suggesting that the *Physcomitrella* PSI–PSII megacomplex contained LHCSR. As LHCSR has been lost in higher plants during plant evolution, the presence of LHCSR in the PSI–PSII megacomplex represents a significant difference in the PSI–PSII megacomplexes of *Physcomitrella* and Arabidopsis. In addition, the immunoblotting analysis (Fig. S3) showed that PsbS co-migrated with the PSI–PSII megacomplex as well in our IpCN-PAGE analysis. The results are consistent with a previous report showing the co-migration of PsbS and the PSI–PSII megacomplex in Arabidopsis (Suorsa et al. 2015). The presence of both LHCSR and PsbS proteins in the PSI–PSII megacomplex implies that they might contribute to dissipating the excess energy in the megacomplex as heat.

Steady-state fluorescence emission spectra of the PSI–PSII megacomplex at 77 K

The PSI–PSII megacomplex separated by IpCN-PAGE (Fig. 1) was further characterized by its steady-state fluorescence emission spectra at 77 K (Fig. 4). Because the individual fluorescence emission spectra of the PSI–LHCI, the PSII–LHCII, and the LHCII trimer are required to analyze the PSI–PSII megacomplex as references, we solubilized the thylakoid protein complexes by α -DM and resolved them with a CN-PAGE standard (Fig. S4). We used α -DM as a detergent in this experiment, as it can solubilize the grana core where the majority of the PSII–LHCII is localized. We observed the PSII–LHCII bands (Fig. S4), which were not clearly shown in the IpCN-PAGE gel, using the digitonin-solubilized protein complexes (Figs. 1, 3). It should be noted that α -DM could inhibit energy transfer from PSII to PSI within the PSI–PSII megacomplex (Supplementary Fig. 14 in Yokono et al. 2015). Thus, digitonin is a better detergent for the solubilization of the PSI–PSII megacomplex.

Fig. 2 Immunoblot analyses of PsbB (PSII), PsbC (PSII), PsaB (PSI), Lhcb2 (LHCII), Lhcb3 (LHCII), and LHCSR proteins after 2D-IPCN/SDS-PAGE of the thylakoid protein complexes in *Physcomitrella* protonemata grown under low-light conditions



Then, we measured the fluorescence emission spectra of the PSI–LHCI, the PSII–LHCII, and the LHCII trimer (Fig. S5). The identification of resolved bands was performed by silver-staining (Fig. S6) and immunoblot analysis using the specific antibodies against PSI, PSII, LHCII, and LHCSR (Fig. S7). The spectra of the *Physcomitrella* PSI–PSII megacomplex (Fig. 4) was found to be very similar to those of the PSI–PSII megacomplex isolated from *Arabidopsis* (Yokono et al. 2015). A large fluorescence peak at approximately 725 nm (Fig. 4) corresponded to low-energy chlorophylls in the PSI–LHCI (Fig. S5). In addition, a much smaller broad peak at approximately 690 nm was observed. As the DM-solubilized PSII–LHCII and LHCII trimer resolved by CN-PAGE showed fluorescence peaks at approximately 693 nm and 678 nm (Fig. S5), the much smaller peak at approximately 690 nm might have been emitted by PSII–LHCII (Fig. 4). These data suggested that the efficient energy transfer from PSII to PSI occurred within the *Physcomitrella* PSI–PSII megacomplex, as observed in *Arabidopsis* (Yokono et al. 2015). The small differences observed in the different fluorescence spectra before and after 1 h of

strong illumination (Fig. 4) implied that the strong illumination induced the *Physcomitrella* PSI–PSII megacomplex to transfer more excitation energy to low-energy chlorophylls in PSI, which may help *Physcomitrella* adapt to strong light conditions (Yokono et al. 2019).

Time-resolved fluorescence of the PSI–PSII megacomplex

To elucidate the fate of the excitation energy absorbed by the PSI–PSII megacomplex, we analyzed the fluorescence kinetics of the PSI–PSII megacomplex before and after 1 h of strong illumination (Fig. 5). The 1 h of illumination appeared to slightly increase the amounts of LHCSR and PsbS proteins (Fig. S8). In addition, 1 h of illumination strongly induced the conversion of violaxanthin to zeaxanthin (Table S1), which is required to achieve a high degree of NPQ in both the LHCSR- and PsbS-dependent pathways in *Physcomitrella* (Pinnola et al. 2013). It has previously been shown that PSII–LHCII supercomplexes with LHCSR have a greater quenching ability at low pH than that at neutral

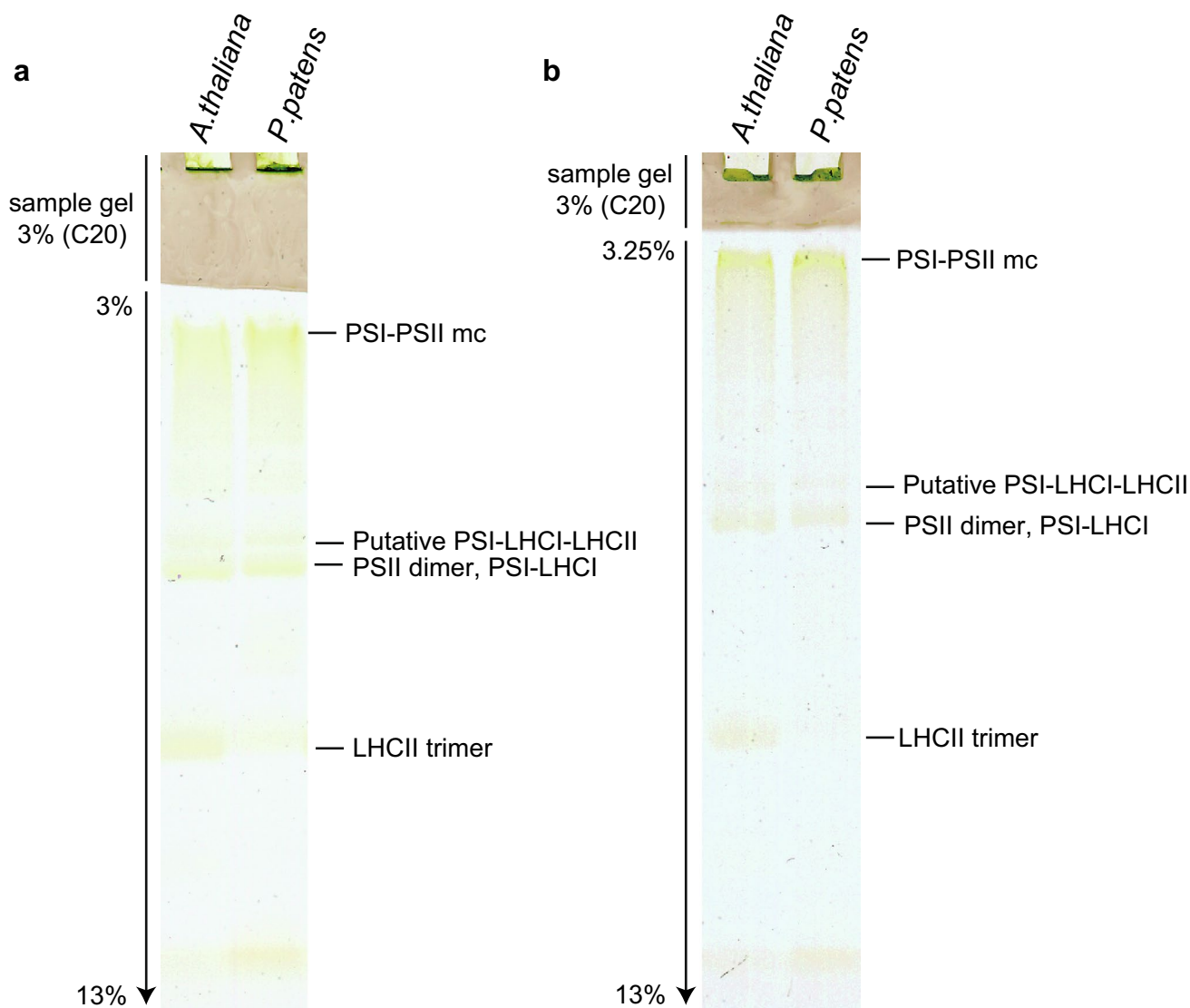


Fig. 3 Separation of the *Arabidopsis* and *Physcomitrella* thylakoid protein complexes by IpCN-PAGE using gels of different acrylamide concentrations (**a** 3–13%; **b** 3.25–13%). Thylakoid protein complexes

were solubilized in 1% digitonin. The sample gel (C20) was made by using an acrylamide solution of 3% T and 20% C (Strecker et al. 2010)

pH in *Chlamydomonas* (Tokutsu and Minagawa 2013). In addition, *Chlamydomonas* LHCSR1 is known to enhance energy transfer from LHCII to PSI at low pH (Kosuge et al. 2018). This implied that the *Physcomitrella* PSI–PSII megacomplex with LHCSR might show greater quenching ability at low pH. To test whether the PSI–PSII megacomplex with LHCSR showed a greater quenching ability at low pH, we measured the bands after soaking them in buffers that were adjusted to neutral pH (pH 7.0) or low pH (pH 4.5). The absorption spectrum of the PSI–PSII megacomplexes was not significantly changed at low pH and under strong light illumination (Fig. S9).

The fluorescence decay-associated spectra of the PSI–PSII megacomplex isolated from the *Physcomitrella*

cells without strong illumination are shown in Fig. 5a. Fluorescence lifetimes are summarized in Table S2. Under neutral pH conditions (Fig. 5a; solid lines), the kinetics were similar to those in the *Arabidopsis* megacomplex (Yokono et al. 2015). The first-lifetime component (~50 ps) reflects the fast energy migration between the PSII core antennae and the PSI core antennae. The fast energy migration between the PSII and the PSI core antennae strongly suggests that the binding between the PSII and the PSI was well-ordered, which also supports our hypothesis that the structure of *Physcomitrella* PSI–PSII megacomplex is similar to that of *Arabidopsis* megacomplex. In addition, the second to fifth components reflect trappings at the reaction centers and low-energy chlorophylls after energy migration. The

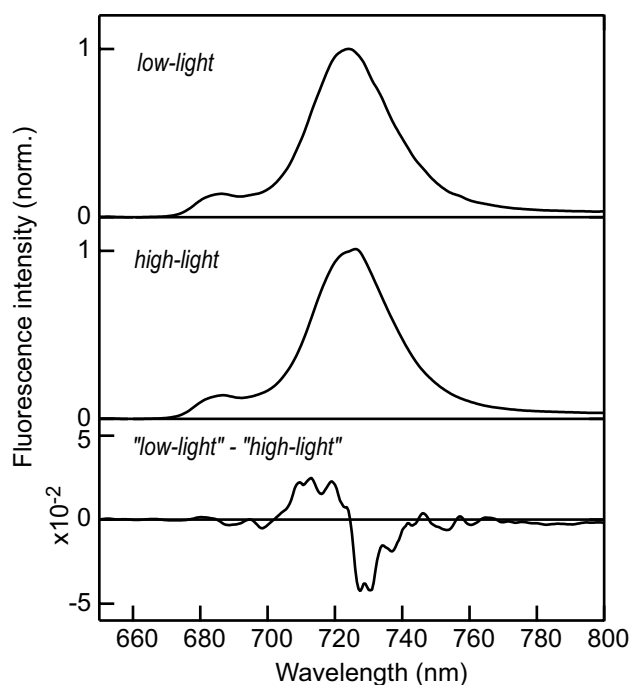


Fig. 4 Steady-state fluorescence spectra of the PSI–PSII megacomplex (Fig. 1). The measurement temperature was 77 K. The upper graph shows the spectrum isolated from thalli grown under low-light conditions; the middle graph shows the spectrum isolated from thalli grown under high light conditions; while the lower graph shows the difference spectrum between the cells grown under low-light-conditions and those illuminated under a strong light

sixth-lifetime component is the delayed fluorescence spectra, which reflects the excitation energy distribution after the direct excitation of the PSII reaction center. A larger peak originated from PSI–LHCI than that from PSII–LHCII in the sixth lifetime, which was suggestive of efficient energy transfer from PSII to PSI within the PSI–PSII megacomplex. The estimated spillover ratio did not show large changes under the different conditions (Table S2), suggesting that the balance of the energy distribution between the two photosystems was regulated without modification of the direct PSI–PSII interaction. This behavior was also observed in the green algae *Chlamydomonas reinhardtii* and *Chlorella variabilis* (Ueno et al. 2018), but not in Arabidopsis (Yokono et al. 2015).

At a low pH, fast fluorescence decay was enhanced at approximately 710 nm (Fig. 5a, second-lifetime component). This tendency became more prominent under strong light growth conditions (Fig. 5b, second-lifetime component), indicating that the enhanced accumulation of zeaxanthin and/or the higher levels of the LHCSR and the PsbS induced fast fluorescence decay. The fluorescence at approximately 710 nm was thought to be emitted by an energy-dissipative state of LHCII and/or PSI (Iwai et al. 2010; Kosuge et al. 2018; Vasil'ev et al. 1997). The fast decrease in the

fluorescence at approximately 710 nm (~200 ps) could be caused by quenching of the energy-dissipative state of LHCII or by the subsequent trapping at the PSI core (Bos et al. 2017; Mimuro et al. 2010). Conversely, the amplitude of the fluorescence at 740 nm, which reflects the trapping of the low-energy chlorophylls in LHCI (Iwai et al. 2015; Mazor et al. 2015) was decreased at low pH (Fig. 5, fifth-lifetime component). This also implies that the energy was dissipated around LHCII and/or was trapped in the PSI core before it reached LHCI. The enhanced 710 nm peak was also observed in the delayed fluorescence spectra (Fig. 5, sixth-lifetime component), reflecting the diversification of the destination of the energy transfer from PSII.

Discussion

Isolation of the PSI–PSII megacomplex with LHCSR in *Physcomitrella* by IpCN-PAGE

In the present study, the PSI–PSII megacomplex in the protonemata of *Physcomitrella* was resolved by the IpCN-PAGE (Figs. 1, 3). The movement of the *Physcomitrella* PSI–PSII megacomplex band through the sample gel showed that the band was not partially solubilized membrane particles, but a huge protein complex (< 10 MDa) (Strecker et al. 2010). The similar migration distance of the *Physcomitrella* PSI–PSII megacomplex to the Arabidopsis megacomplex in IpCN-PAGE (Fig. 3) showed that these complexes are similar in size (Yokono et al. 2019). We recently proposed the first structural model of the Arabidopsis PSI–PSII megacomplex that consists of one PSII dimer sandwiched between two PSI–LHCI complexes with the additional LHCII trimers surrounded peripherally, based on the negatively stained EM particles (Yokono et al. 2019). The similarities in molecular size, the 77 K steady-state fluorescence spectra (Fig. 4), and the fluorescence kinetics (Fig. 5) of the *Physcomitrella* PSI–PSII megacomplex to the Arabidopsis megacomplex strongly suggest that the molecular structures of the *Physcomitrella* PSI–PSII and Arabidopsis megacomplexes are similar (Yokono et al. 2019). However, further studies will be required to confirm this.

In addition, fast energy transfer occurred from the PSII to PSI cores in the *Physcomitrella* PSI–PSII megacomplex (Fig. 5, first-lifetime component), which suggests a direct interaction between the PSII and PSI cores (Yokono and Akimoto 2018; Yokono et al. 2015). It should be noted that only the co-migration of the PSII and the PSI did not show energy transfer between them as seen in our previous data (w2 and w3 bands shown in Fig. 1c in Yokono et al. 2015), suggesting that a well-ordered assembly of the PSI–PSII megacomplex is essential for achieving a rapid energy transfer from PSII to PSI (Fig. 5).

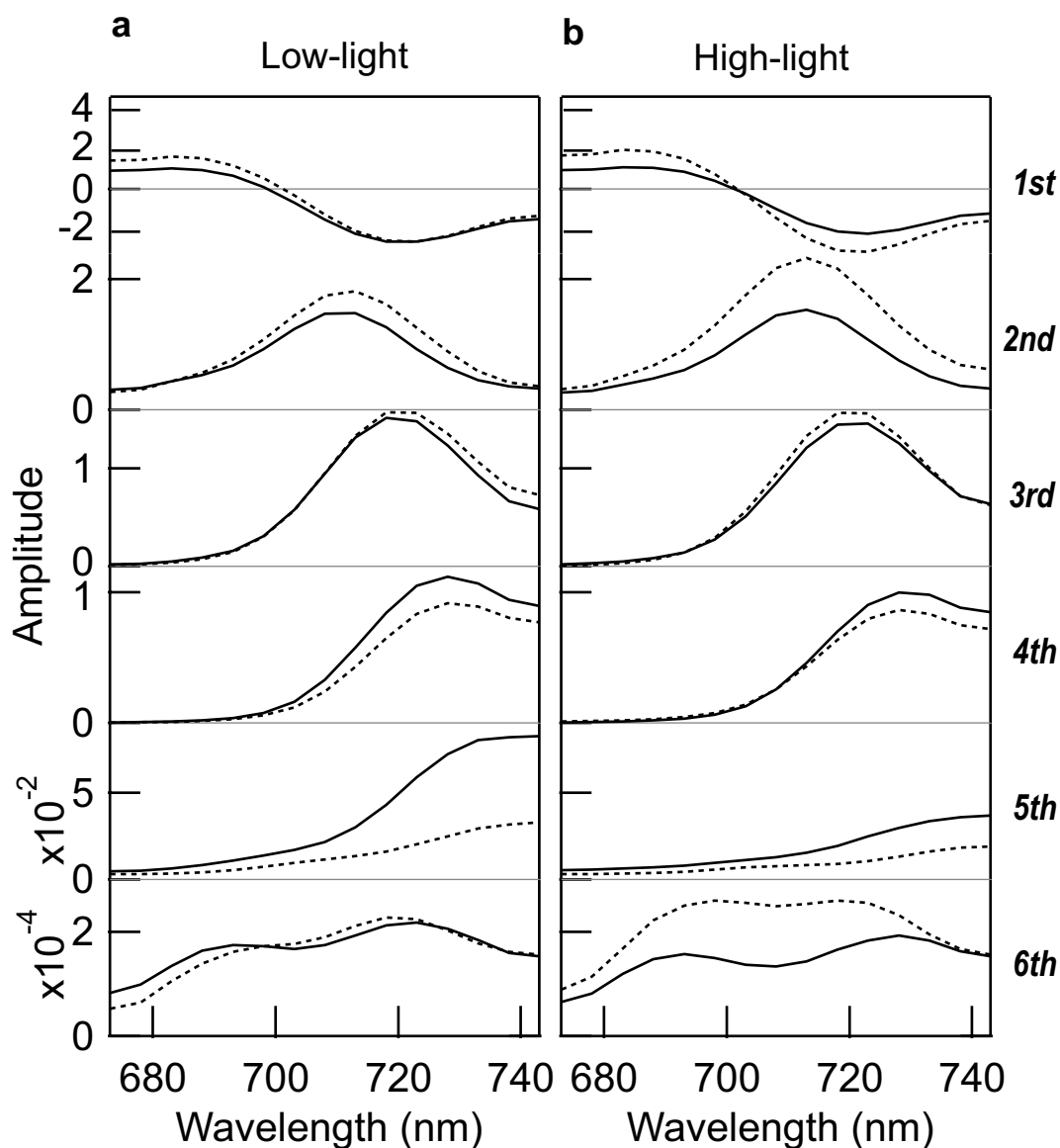


Fig. 5 Fluorescence decay-associated spectra of PSI–PSII megacomplex isolated from **a** low light-grown cell and **b** high light grown cell. Solid line (pH 7), dotted line (pH 4.5). Measurement temperature was 77 K. Lifetimes are summarized in Table S2

In addition to the PSI, PSII, and LHCs that are also found in the Arabidopsis PSI–PSII megacomplexes, the *Physcomitrella* PSI–PSII megacomplex contained LHCSR, which plays an important role in the protection of photosystems by dissipating excess energy in *Chlamydomonas* (Peers et al. 2009) and *Physcomitrella* (Alboresi et al. 2010). The co-migration of PSII–LHCII with LHCSR was also observed by CN-PAGE (Fig. S7), suggesting that LHCSR associates not only with the PSI–PSII megacomplex but also with the PSII–LHCII megacomplex in *Physcomitrella* (Fig. S7). Furthermore, we also found the presence of PsbS in the *Physcomitrella* PSI–PSII megacomplex (Fig. S3). This finding is consistent with a previous report that PsbS is included in the

Arabidopsis PSI–PSII megacomplex (Suorsa et al. 2015). The presence of LHCSR and PsbS in the *Physcomitrella* PSI–PSII megacomplex implies that heat dissipation of the excitation energy absorbed by them plays an important role in mitigating photo-oxidative damage in the megacomplex.

pH-dependent quenching in the PSI–PSII megacomplex

At low pH conditions, fast trapping (~ 200 ps) at approximately 710 nm was enhanced and, concomitantly, trapping at low-energy chlorophylls in LHCI (740 nm) was suppressed (Fig. 5). We assumed that the fast decay in the chlorophyll

fluorescence at approximately 710 nm originated from the energy-dissipative state of LHCII and/or by subsequent trapping at the PSI core. The energy transfer rate from the PSII core to the PSI core was not altered, even at low pH (first lifetime component (~50 ps) in Fig. 5). This implied that the enhancement of fast trapping at approximately 710 nm was not responsible for the change in the PSI core itself in response to the low pH conditions but was responsible for the change in the peripheral LHCII in the PSI–PSII megacomplex of *Physcomitrella*. It should be noted that the existence of an energy transfer pathway from LHCII to PSI that does not involve LHCI has already been reported (Benson et al. 2015; Ferroni et al. 2018). If an additional quenching site is activated in the peripheral LHCII at a low pH, it will accept energy from the PSI core.

A recent study suggested that LHCSR might bind to LHCII in PSI–LHCI/II in *Physcomitrella* (Pinnola et al. 2015) and that LHCSR mediates pH-dependent quenching (Pinnola et al. 2017; Tokutsu and Minagawa 2013). Pinnola et al. (2015) suggested that LHCSR does not directly quench PSI–LHCI, but instead quench it by modulating the lifetime of an LHCII population (Pinnola et al. 2015, 2017). Moreover, *Chlamydomonas* cells that possessed both LHCII and LHCSR exhibited a 710-nm fluorescence maximum at 77 K and displayed pH-dependent quenching (Dinc et al. 2016). Combined with these data, we suggested that LHCSR binds to peripheral LHCII in the *Physcomitrella* PSI–PSII megacomplex and quenches the excitation energy via a pH- or zeaxanthin-dependent manner.

In addition to LHCSR, previous studies showed that PsbS also binds to LHCII in the PSII–LHCII and contributes to forming NPQ in both a pH- and a zeaxanthin-dependent manner (Correa-Galvis et al. 2016a, b; Sacharz et al. 2017). Thus, it is possible to speculate that both LHCSR and PsbS can contribute the pH-dependent quenching in the *Physcomitrella* megacomplex.

***P. patens* utilization of shallower low-energy chlorophylls**

Plants possess various low-energy chlorophylls in the PSI–LHCI. In the fluorescence decay-associated spectrum of the *Physcomitrella* PSI–PSII megacomplex (Fig. 5), fluorescence at 710 nm, 720 nm, 730 nm, and 740 nm was detected in the second to fifth-lifetime components (summarized in Table 1), respectively. Meanwhile, the *Arabidopsis* PSI–PSII megacomplex showed fluorescence peaks at 720 nm, 725 nm, 735 nm, and 740 nm (Fig. S3b in Yokono et al. (2015)). The difference in the composition of the low-energy chlorophylls between *Arabidopsis* and *Physcomitrella* might reflect the variations in the LHCI proteins in *Physcomitrella* (Busch et al. 2013).

Table 1 The amplitude ratio of low-energy chlorophylls

Peak wavelength	Lifetime	Amplitude	Amplitude ratio (%)	Deeper ratio (%)
<i>Physcomitrella patens</i>				
710 nm	200 ps	1.5	36	28
720 nm	750 ps	1.5	36	
730 nm	1.9 ns	1.1	26	
740 nm	4.1 ns	0.08	2	
<i>Arabidopsis thaliana</i> [from Yokono et al. (2015)]				
720 nm	240 ps	0.35	28	72
725 nm	1.0 ns	0.26	20	
735 nm	2.2 ns	0.44	35	
740 nm	3.3 ns	0.22	17	

From a functional perspective, low-energy chlorophylls are classified into two types, shallower and deeper low-energy chlorophylls, depending on their energy levels. In the green lineage, the PSI core possesses shallower low-energy chlorophylls, whereas LHCI possesses deeper low-energy chlorophylls (Kunugi et al. 2016). Typically, shallower low-energy chlorophylls show fluorescence maxima at approximately 720 nm or shorter and possess a large Förster overlap integral at P700. They can transfer excitation energy to P700 via the uphill energy transfer process (Melkozernov and Blankenship 2005; Melkozernov et al. 2004). Conversely, deeper low-energy chlorophylls in PSI–LHCI can dissipate excitation energy as heat by the following two mechanisms (reviewed by Yokono and Akimoto 2018). The first mechanism depends on their ability to transfer excitation energy to P700⁺ (Schlodder et al. 2011; Shubin et al. 1995). Their fluorescence maxima of approximately 725 nm or longer enables them to possess a large Förster overlap integral at P700⁺. Since P700⁺ is an excellent quencher (Croce and van Amerongen 2013), their ability to transfer energy to P700⁺ should contribute to the dissipation of excess energy as heat.

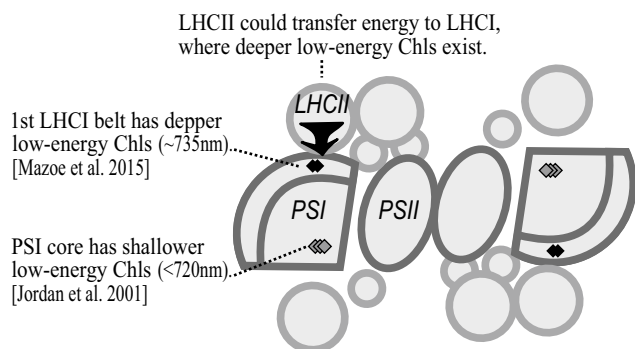
The second mechanism depends on their ability to form a charge-transfer state with a carotenoid, which also enables them to dissipate excess energy as heat (Ballottari et al. 2014). Owing to these two mechanisms, PSI–LHCI tends to tolerate high levels of illumination as it has deeper low-energy chlorophylls (Yokono et al. 2019). Both *Physcomitrella* and *Arabidopsis* possess shallower and deeper low-energy chlorophylls. In the *Physcomitrella* PSI–PSII megacomplex, 72% of the amplitude was occupied by the shallower low-energy chlorophylls, whereas in the *Arabidopsis* PSI–PSII megacomplex, 72% of the amplitude was occupied by the deeper low-energy chlorophylls (Table 1). The amplitude reflects the probability of energy acceptance of each low-energy chlorophyll. Therefore, the excitation energy absorbed by *Physcomitrella* PSI–PSII was mainly

transferred to P700 to perform photosynthesis, and the heat-dissipation processes may show lower efficiency depending on the deeper low-energy chlorophylls. In contrast, the excitation energy absorbed by Arabidopsis PSI–PSII was primarily dissipated as heat rather than being utilized for photosynthesis. The difference between *Physcomitrella* and Arabidopsis might be related to the structural differences in PSI–LHCI. Arabidopsis PSI–LHCI possesses one layer of the LHCI belt containing four Lhca proteins, which are all in the range of the Förster critical distance from P700⁺ (<80–90 Å) (Mazor et al. 2015; van Grondelle 1985). Therefore, all the deeper low-energy chlorophylls in the LHCI belt in Arabidopsis might participate in the energy transfer to P700⁺ to dissipate the excitation energy (Yokono and Akimoto 2018). Conversely, *Physcomitrella* possesses two layers of the LHCI belt containing eight Lhca proteins (Iwai et al. 2018), although the second layer may be beyond the range of the Förster critical distance. Thus, even if the second layer of the LHCI belt possesses the deeper low-energy chlorophylls, they may not efficiently perform P700⁺-dependent quenching. Alternatively, *Physcomitrella* possesses LHCSR and PsbS that could bind to the peripheral LHCII around PSI–LHCI (Pinnola et al. 2015, 2017) and PSII–LHCII (Correa-Galvis et al. 2016a, b; Sacharz et al. 2017) and act as a quencher that possibly works with shallower low-energy chlorophylls.

Possible photoprotection strategy in *P. patens*

In *Physcomitrella*, the shallower low-energy chlorophylls can efficiently transfer absorbed energy to P700 to perform photosynthesis (Yokono and Akimoto 2018). When the light becomes strong, *Physcomitrella* induces the accumulation of PsbS and LHCSR proteins (Gerotto et al. 2011). Recent studies have shown that *Chlamydomonas* LHCSR proteins are induced by blue light (Petroutsos et al. 2016) and UV (Allorent et al. 2016; Tilbrook et al. 2016; Tokutsu et al. 2019). If mosses possess similar mechanisms to induce LHCSR proteins in response to blue light and UV, this should contribute to their adaptation to terrestrial environments. However, PsbS localizes in the grana stack and can dissipate the excitation energy that is absorbed by PSII–LHCII as heat (Pinnola et al. 2015). Thus, under high levels of illumination, linear electron transfer is suppressed by the PsbS-dependent NPQ and can be reduced in favor of cyclic electron flow (Allahverdiyeva et al. 2015). P700⁺ may accumulate within the PSI–PSII megacomplex in the grana margin and excitation energy trapped by the deeper low-energy chlorophylls in the PSI–PSII megacomplex is efficiently dissipated by P700⁺. This scenario is likely occurring in Arabidopsis (Fig. 6). However, the energy transfer capacity of the deeper low-energy chlorophylls was limited in *Physcomitrella* (Fig. 5, Table S2). Instead,

Arabidopsis thaliana



Physcomitrella patens

Additional shallower low-energy Chls may exist in the additional LHCII under high-light condition. Energy can be quenched by LHCSR. [Bonente et al. 2011, Kondo et al. 2017].

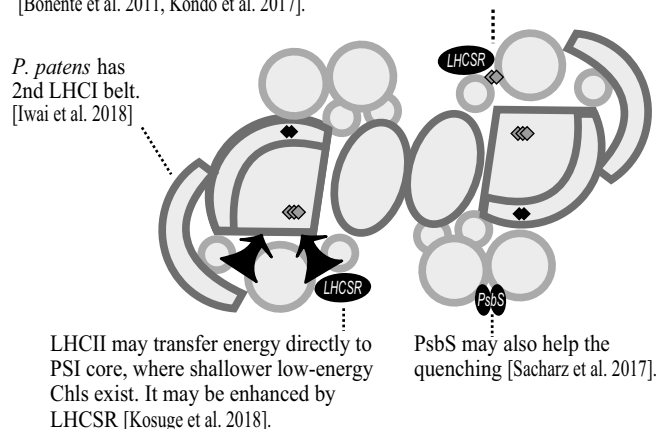


Fig. 6 Schematic model of the PSI–PSII megacomplex in Arabidopsis and *Physcomitrella*. The large and small circles represent the LHCII trimer and monomer, respectively. If the energy was trapped by the deeper low-energy chlorophylls (Chls), it could be dissipated efficiently. However, if the energy was trapped by the shallower low-energy Chls, uphill energy transfer occurred to P700 under physiological temperatures, and the energy could then be utilized for photosynthesis. In Arabidopsis, the PSI core has shallower low-energy Chls, whereas the LHCI belt has deeper low-energy Chls. Digitonin-sensi-

tive LHCII could transfer energy to the PSI core via LHCI (Benson et al. 2015). In contrast, the PSI in *Physcomitrella* has a second LHCI belt, which was not found in Arabidopsis, in addition to the first LHCI belt. Shallower low-energy Chls may exist in the additional LHCII of the *Physcomitrella* PSI–PSII megacomplex, which might transfer energy directly to the PSI core. Differences in the LHCII binding sites may affect the course of the excitation energy. Under strong light conditions, LHCSR in the *Physcomitrella* PSI–PSII megacomplex probably dissipates the excitation energy

LHCSR can dissipate the excitation energy trapped by PSI (Pinnola et al. 2015), which may help survive in strong light conditions. The 710 nm chlorophylls in the putative peripheral LHCI of the *Physcomitrella* PSI–PSII megacomplex might shift the energy distribution toward the quenching site, which may enhance energy dissipation efficiency under low pH conditions (Yokono et al. 2018). This hypothetical scheme should work well under high light conditions (Fig. 6), although further studies are required to verify this hypothesis.

One limitation of this study is that no information was obtained on how changes in the PSI–PSII megacomplex related to the developmental stages of *Physcomitrella*. Future studies, including the comparison of the PSI–PSII megacomplex in the protonemata and gametophore, will be important for understanding the function of PSI–PSII megacomplex in the developmental of *Physcomitrella*.

Conclusion

In this study, we isolated a *Physcomitrella* PSI–PSII megacomplex, which is also present in *Arabidopsis thaliana* (Yokono et al. 2015), *Selaginella martensii* (Ferroni et al. 2016), and *Neochloris oleoabundans* (Giovanardi et al. 2017). The presence of the PSI–PSII megacomplex in these green plants suggests that the PSI–PSII megacomplex is widely prevalent among land plants. However, the presence of LHCSR in the *Physcomitrella* PSI–PSII megacomplex is unique and does not occur in *Arabidopsis*. Given the molecular and physiological function of LHCSR, the LHCSR, together with PsbS in the megacomplex might assist in dissipating excess light energy as heat. We also observed that the chlorophyll fluorescence spectra with a peak of 710 nm were enhanced under low pH conditions—something that was not observed in the *Arabidopsis* PSI–PSII megacomplex. This observation can be explained by assuming that LHCSR and/or PsbS bind at the additional LHCI that was not present in the *Arabidopsis* PSI–PSII megacomplex and enhances heat dissipation under the high light illumination.

In conclusion, our results from this study provide new insights into the regulation of photosynthesis in response to light conditions in *Physcomitrella*.

Acknowledgements This work was supported by JSPS (Japan Society for the Promotion of Science) KAKENHI Grant numbers 23770035 to A. Takabayashi, 16H06553 to S. Akimoto, and 16H06554 to R. Tanaka.

Compliance with ethical standards

Conflict of interest The authors declare that they have no conflict of interest.

References

- Alboresi A, Gerotto C, Giacometti GM, Bassi R, Morosinotto T (2010) *Physcomitrella patens* mutants affected on heat dissipation clarify the evolution of photoprotection mechanisms upon land colonization. *Proc Natl Acad Sci USA* 107:11128–11133. <https://doi.org/10.1073/pnas.1002873107>
- Allahverdiyeva Y, Suorsa M, Tikkanen M, Aro EM (2015) Photoprotection of photosystems in fluctuating light intensities. *J Exp Bot* 66:2427–2436. <https://doi.org/10.1093/jxb/eru463>
- Allont G, Lefebvre-Legendre L, Chappuis R, Kuntz M, Truong TB, Niyogi KK, Ulm R, Goldschmidt-Clermont M (2016) UV-B photoreceptor-mediated protection of the photosynthetic machinery in *Chlamydomonas reinhardtii*. *Proc Natl Acad Sci USA* 113:14864–14869. <https://doi.org/10.1073/pnas.1607695114>
- Ballottari M, Alcocer MJ, D'Andrea C, Viola D, Ahn TK, Petrosza A, Polli D, Fleming GR, Cerullo G, Bassi R (2014) Regulation of photosystem I light-harvesting by zeaxanthin. *Proc Natl Acad Sci USA* 111:E2431–E2438. <https://doi.org/10.1073/pnas.1404377111>
- Bellaïf S, Barneche F, Peltier G, Rochaix JD (2005) State transitions and light adaptation require chloroplast thylakoid protein kinase STN7. *Nature* 433:892–895. <https://doi.org/10.1038/nature03286>
- Benson SL, Maheswaran P, Ware MA, Hunter CN, Horton P, Jansson S, Ruban AV, Johnson MP (2015) An intact light-harvesting complex I antenna system is required for complete state transitions in *Arabidopsis*. *Nat Plant* 1:15176. <https://doi.org/10.1038/nplants.2015.176>
- Bonente G, Ballottari M, Truong TB, Morosinotto T, Ahn TK, Fleming GR, Niyogi KK, Bassi R (2011) Analysis of LhcSR3, a protein essential for feedback de-excitation in the green alga *Chlamydomonas reinhardtii*. *PLOS Biol* 9:e1000577. <https://doi.org/10.1371/journal.pbio.1000577>
- Bos I, Bland KM, Tian LJ, Croce R, Frankel LK, van Amerongen H, Bricker TM, Wientjes E (2017) Multiple LHCI antennae can transfer energy efficiently to a single photosystem I. *Biochim Biophys Acta* 1858:371–378. <https://doi.org/10.1016/j.bbabi.2017.02.012>
- Busch A, Petersen J, Webber-Birungi MT, Powikrowska M, Lassen LM, Naumann-Busch B, Nielsen AZ, Ye J, Boekema EJ, Jensen ON, Lunde C, Jensen PE (2013) Composition and structure of photosystem I in the moss *Physcomitrella patens*. *J Exp Bot* 64:2689–2699. <https://doi.org/10.1093/jxb/ert126>
- Correa-Galvis V, Poschmann G, Melzer M, Stühler K, Jahns P (2016a) PsbS interactions involved in the activation of energy dissipation in *Arabidopsis*. *Nat Plants* 2:15225. <https://doi.org/10.1038/nplants.2015.225>
- Correa-Galvis V, Redekop P, Guan K, Griess A, Truong TB, Wakao S, Niyogi KK, Jahns P (2016b) Photosystem II subunit PsbS is involved in the induction of LHCSR protein-dependent energy dissipation in *Chlamydomonas reinhardtii*. *J Biol Chem* 291:17478–17487. <https://doi.org/10.1074/jbc.M116.737312>
- Croce R, van Amerongen H (2013) Light-harvesting in photosystem I. *Photosynth Res* 116:153–166. <https://doi.org/10.1007/s1120-013-9838-x>
- Dinc E, Tian L, Roy LM, Roth R, Goodenough U, Croce R (2016) LHCSR1 induces a fast and reversible pH-dependent fluorescence quenching in LHCI in *Chlamydomonas reinhardtii* cells. *Proc Natl Acad Sci USA* 113(27):7673–7678. <https://doi.org/10.1073/pnas.1605380113>
- Ferroni L, Suorsa M, Aro EM, Baldisserotto C, Pancaldi S (2016) Light acclimation in the lycophyte *Selaginella martensii* depends on changes in the number of photosystems and on the

- flexibility of the light-harvesting complex II antenna association with both photosystems. *New Phytol* 211:554–568. <https://doi.org/10.1111/nph.13939>
- Ferroni L, Cucuzza S, Angeleri M, Aro EM, Pagliano C, Giovanardi M, Baldisserotto C, Pancaldi S (2018) In the lycophyte *Selaginella martensii* is the “extra-qT” related to energy spillover? Insights into photoprotection in ancestral vascular plants. *Environ Exp Bot* 154:110–122. <https://doi.org/10.1016/j.envexpbot.2017.10.023>
- Gerotto C, Alboresi A, Giacometti GM, Bassi R, Morosinotto T (2011) Role of PSBS and LHCSR in *Physcomitrella patens* acclimation to high light and low temperature. *Plant Cell Environ* 34:922–932. <https://doi.org/10.1111/j.1365-3040.2011.02294.x>
- Giovanardi M, Poggioli M, Ferroni L, Lespinasse M, Baldisserotto C, Aro EM, Pancaldi S (2017) Higher packing of thylakoid complexes ensures a preserved photosystem II activity in mixotrophic *Neochloris oleoabundans*. *Algal Res* 25:322–332. <https://doi.org/10.1016/j.algal.2017.05.020>
- Goss R, Lepetit B (2015) Biodiversity of NPQ. *J Plant Physiol* 172:13–32. <https://doi.org/10.1016/j.jplph.2014.03.004>
- Iwai M, Yokono M (2017) Light-harvesting antenna complexes in the moss *Physcomitrella patens*: implications for the evolutionary transition from green algae to land plants. *Curr Opin Plant Biol* 37:94–101. <https://doi.org/10.1016/j.pbi.2017.04.002>
- Iwai M, Yokono M, Inada N, Minagawa J (2010) Live-cell imaging of photosystem II antenna dissociation during state transitions. *Proc Natl Acad Sci USA* 107:2337–2342. <https://doi.org/10.1073/pnas.0908808107>
- Iwai M, Yokono M, Kono M, Noguchi K, Akimoto S, Nakano A (2015) Light-harvesting complex Lhcb9 confers a green alga-type photosystem I supercomplex to the moss *Physcomitrella patens*. *Nat Plants* 1:14008. <https://doi.org/10.1038/nplants.2014.8>
- Iwai M, Grob P, Iavarone AT, Nogales E, Niyogi KK (2018) A unique supramolecular organization of photosystem I in the moss *Physcomitrella patens*. *Nat Plants* 4:904–909. <https://doi.org/10.1038/s41477-018-0271-1>
- Järvi S, Suorsa M, Paakkarinen V, Aro EM (2011) Optimized native gel systems for separation of thylakoid protein complexes: novel super- and mega-complexes. *Biochem J* 439:207–214. <https://doi.org/10.1042/BJ20102155>
- Kondo T, Pinnola A, Chen WJ, Dall’Osto L, Bassi R, Schlau-Cohen GS (2017) Single-molecule spectroscopy of LHCSR1 protein dynamics identifies two distinct states responsible for multi-timescale photosynthetic photoprotection. *Nat Chem* 9:772–778. <https://doi.org/10.1038/nchem.2818>
- Kosuge K, Tokutsu R, Kim E, Akimoto S, Yokono M, Ueno Y, Minagawa J (2018) LHCSR1-dependent fluorescence quenching is mediated by excitation energy transfer from LHCI to photosystem I in *Chlamydomonas reinhardtii*. *Proc Natl Acad Sci USA* 115:3722–3727. <https://doi.org/10.1073/pnas.1720574115>
- Kunugi M, Satoh S, Ihara K, Shibata K, Yamagishi Y, Kogame K, Obokata J, Takabayashi A, Tanaka A (2016) Evolution of green plants accompanied changes in light-harvesting systems. *Plant Cell Physiol* 57:1231–1243. <https://doi.org/10.1093/pcp/pcw071>
- Mazor Y, Borovikova A, Nelson N (2015) The structure of plant photosystem I super-complex at 2.8 Å resolution. *Elife* 4:e07433. <https://doi.org/10.7554/eLife.07433>
- Melkozernov AN, Blankenship RE (2005) Structural and functional organization of the peripheral light-harvesting system in photosystem I. *Photosynth Res* 85:33–50. <https://doi.org/10.1007/s11120-004-6474-5>
- Melkozernov AN, Kargul J, Lin S, Barber J, Blankenship RE (2004) Energy coupling in the PSI–LHCI supercomplex from the green alga *Chlamydomonas reinhardtii*. *J Phys Chem B* 108:10547–10555. <https://doi.org/10.1021/jp049375n>
- Mimuro M, Yokono M, Akimoto S (2010) Variations in photosystem I properties in the primordial cyanobacterium *Gloeobacter violaceus* PCC 7421. *Photochem Photobiol* 86:62–69. <https://doi.org/10.1111/j.1751-1097.2009.00619.x>
- Minagawa J, Tokutsu R (2015) Dynamic regulation of photosynthesis in *Chlamydomonas reinhardtii*. *Plant J* 82:413–428. <https://doi.org/10.1111/tpj.12805>
- Nishiyama T, Hiwatashi Y, Sakakibara I, Kato M, Hasebe M (2000) Tagged mutagenesis and gene-trap in the moss, *Physcomitrella patens* by shuttle mutagenesis. *DNA Res* 7:9–17. <https://doi.org/10.1093/dnares/7.1.9>
- Niyogi KK, Truong TB (2013) Evolution of flexible non-photochemical quenching mechanisms that regulate light harvesting in oxygenic photosynthesis. *Curr Opin Plant Biol* 16:307–314. <https://doi.org/10.1016/j.pbi.2013.03.011>
- Peers G, Truong TB, Ostendorf E, Busch A, Elrad D, Grossman AR, Hippler M, Niyogi KK (2009) An ancient light-harvesting protein is critical for the regulation of algal photosynthesis. *Nature* 462:518–521. <https://doi.org/10.1038/nature08587>
- Pesaresi P, Hertle A, Pribil M, Kleine T, Wagner R, Strissel H, Ihnatowicz A, Bonardi V, Scharfenberg M, Schneider A, Pfanschmidt T, Leister D (2009) Arabidopsis STN7 kinase provides a link between short- and long-term photosynthetic acclimation. *Plant Cell* 21:2402–2423. <https://doi.org/10.1105/tpc.108.064964>
- Petroutsos D, Tokutsu R, Maruyama S, Flori S, Greiner A, Magneschi L, Cusant L, Kottke T, Mittag M, Hegemann P, Finazzi G, Minagawa J (2016) A blue-light photoreceptor mediates the feedback regulation of photosynthesis. *Nature* 537:563–566. <https://doi.org/10.1038/nature19358>
- Pinnola A, Dall’Osto L, Gerotto C, Morosinotto T, Bassi R, Alboresi A (2013) Zeaxanthin binds to light-harvesting complex stress-related protein to enhance nonphotochemical quenching in *Physcomitrella patens*. *Plant Cell* 25:3519–3534. <https://doi.org/10.1105/tpc.113.114538>
- Pinnola A, Cazzaniga S, Alboresi A, Nevo R, Levin-Zaidman S, Reich Z, Bassi R (2015) Light-harvesting complex stress-related proteins catalyze excess energy dissipation in both photosystems of *Physcomitrella patens*. *Plant Cell* 27:3213–3227. <https://doi.org/10.1105/tpc.15.00443>
- Pinnola A, Ballottari M, Bargigia I, Alcocer M, D’Andrea C, Cerullo G, Bassi R (2017) Functional modulation of LHCSR1 protein from *Physcomitrella patens* by zeaxanthin binding and low pH. *Sci Rep* 7:11158. <https://doi.org/10.1038/s41598-017-11101-7>
- Popot JL, Althoff T, Bagnard D, Baneres JL, Bazzacco P, Billon-Denis E, Catoire LJ, Champeil P, Charvolin D, Cocco MJJ, Cremel G, Dahmane T, de la Maza LM, Ebel C, Gabel F, Giusti F, Gohon Y, Goormaghtigh E, Guittet E, Kleinschmidt JH, Kuhlbrandt W, Le Bon C, Martinez KL, Picard M, Pucci B, Sachs JN, Tribet C, van Heijenoort C, Wien F, Zito F, Zoonens M (2011) Amphipols from A to Z. *Annu Rev Biophys* 40:379–408. <https://doi.org/10.1146/annurev-biophys-042910-155219>
- Ruban AV (2015) Evolution under the sun: optimizing light harvesting in photosynthesis. *J Exp Bot* 66:7–23. <https://doi.org/10.1093/jxb/eru400>
- Ruban AV (2016) Nonphotochemical chlorophyll fluorescence quenching: mechanism and effectiveness in protecting plants from photodamage. *Plant Physiol* 170:1903–1916. <https://doi.org/10.1104/pp.15.01935>
- Sacharz J, Giovagnetti V, Ungerer P, Mastroianni G, Ruban AV (2017) The xanthophyll cycle affects reversible interactions between PsbS and light-harvesting complex II to control non-photochemical quenching. *Nat Plants* 3:16225. <https://doi.org/10.1038/nplants.2016.225>
- Schlodder E, Hussels M, Çetin M, Karapetyan NV, Brecht M (2011) Fluorescence of the various red antenna states in photosystem I complexes from cyanobacteria is affected differently by the redox state of P700. *Biochim Biophys Acta* 1807:1423–1431. <https://doi.org/10.1016/j.bbabi.2011.06.018>

- Shubin VV, Bezsmertnaya IN, Karapetyan NV (1995) Efficient energy-transfer from the long-wavelength antenna chlorophylls to P700 in photosystem-I complexes from *Spirulina platensis*. *J Photochem Photobiol B* 30:153–160. [https://doi.org/10.1016/1011-1344\(95\)07173-Y](https://doi.org/10.1016/1011-1344(95)07173-Y)
- Strecker V, Wumaier Z, Wittig I, Schägger H (2010) Large pore gels to separate mega protein complexes larger than 10 MDa by blue native electrophoresis: isolation of putative respiratory strings or patches. *Proteomics* 10:3379–3387. <https://doi.org/10.1002/pmic.201000343>
- Suorsa M, Rantala M, Danielsson R, Jarvi S, Paakkanen V, Schroder WP, Styring S, Mamedov F, Aro EM (2014) Dark-adapted spinach thylakoid protein heterogeneity offers insights into the photosystem II repair cycle. *Biochim Biophys Acta* 1837:1463–1471. <https://doi.org/10.1016/j.bbabi.2013.11.014>
- Suorsa M, Rantala M, Mamedov F, Lespinasse M, Trotta A, Grieco M, Vuorio E, Tikkanen M, Jarvi S, Aro EM (2015) Light acclimation involves dynamic re-organization of the pigment-protein megacomplexes in non-appressed thylakoid domains. *Plant J* 84:360–373. <https://doi.org/10.1111/tpj.13004>
- Tilbrook K, Dubois M, Crocco CD, Yin R, Chappuis R, Allorent G, Schmid-Siebert E, Goldschmidt-Clermont M, Ulm R (2016) UV-B perception and acclimation in *Chlamydomonas reinhardtii*. *Plant Cell* 28:966–983. <https://doi.org/10.1105/tpc.15.00287>
- Tokutsu R, Minagawa J (2013) Energy-dissipative supercomplex of photosystem II associated with LHCSR3 in *Chlamydomonas reinhardtii*. *Proc Natl Acad Sci USA* 110:10016–10021. <https://doi.org/10.1073/pnas.1222606110>
- Tokutsu R, Fujimura-Kamada K, Yamasaki T, Matsuo T, Minagawa J (2019) Isolation of photoprotective signal transduction mutants by systematic bioluminescence screening in *Chlamydomonas reinhardtii*. *Sci Rep* 9:2820. <https://doi.org/10.1038/s41598-019-39785-z>
- Ueno Y, Aikawa S, Kondo A, Akimoto S (2018) Adaptation of light-harvesting functions of unicellular green algae to different light qualities. *Photosynth Res* 139:145–154. <https://doi.org/10.1007/s11120-018-0523-y>
- Umetani I, Kunugi M, Yokono M, Takabayashi A, Tanaka A (2018) Evidence of the supercomplex organization of photosystem II and light-harvesting complexes in *Nannochloropsis granulata*. *Photosynth Res* 136:49–61. <https://doi.org/10.1007/s11120-017-0438-z>
- Van Grondelle R (1985) Excitation-energy transfer, trapping and annihilation in photosynthetic systems. *Biochim Biophys Acta* 811:147–195. [https://doi.org/10.1016/0304-4173\(85\)90017-5](https://doi.org/10.1016/0304-4173(85)90017-5)
- Vasil'ev S, Irrgang KD, Schrotter T, Bergmann A, Eichler HJ, Renger G (1997) Quenching of chlorophyll a fluorescence in the aggregates of LHCII: steady-state fluorescence and picosecond relaxation kinetics. *Biochemistry* 36:7503–7512. <https://doi.org/10.1021/bi9625253>
- Watanabe A, Kim E, Burton-Smith RN, Tokutsu R, Minagawa J (2019) Amphipol-assisted purification method for the highly active and stable photosystem II supercomplex of *Chlamydomonas reinhardtii*. *FEBS Lett* 593:1072–1079. <https://doi.org/10.1002/1873-3468.13394>
- Wobbe L, Bassi R, Kruse O (2016) Multi-level light capture control in plants and green algae. *Trends Plant Sci* 21:55–68. <https://doi.org/10.1016/j.tplants.2015.10.004>
- Xu DQ, Chen Y, Chen GY (2015) Light-harvesting regulation from leaf to molecule with the emphasis on rapid changes in antenna size. *Photosynth Res* 124:137–158. <https://doi.org/10.1007/s11120-015-0115-z>
- Yokono M, Akimoto S (2018) Energy transfer and distribution in photosystem super/megacomplexes of plants. *Curr Opin Biotechnol* 54:50–56. <https://doi.org/10.1016/j.copbio.2018.01.001>
- Yokono M, Takabayashi A, Akimoto S, Tanaka A (2015) A megacomplex composed of both photosystem reaction centres in higher plants. *Nat Commun*. <https://doi.org/10.1038/ncomms7675>
- Yokono M, Umetani I, Takabayashi A, Akimoto S, Tanaka A (2018) Regulation of excitation energy in *Nannochloropsis* photosystem II. *Photosynth Res* 139:155–161. <https://doi.org/10.1007/s11120-018-0510-3>
- Yokono M, Takabayashi A, Kishimoto J, Fujita T, Iwai M, Murakami A, Akimoto S, Tanaka A (2019) The PSI–PSII megacomplex in green plants. *Plant Cell Physiol* accepted. <https://doi.org/10.1093/pcp/pcz026>

Publisher's Note Springer Nature remains neutral with regard to jurisdictional claims in published maps and institutional affiliations.